Evaluation of Right Ventricular Regional Perfusion with Technetium-99m-Sestamibi SPECT

E. Gordon DePuey*, Margie E. Jones, and Ernest V. Garcia

Department of Radiology, Division of Nuclear Medicine, Emory University School of Medicine, Atlanta, Georgia

To evaluate technetium-99m-sestamibi as a right ventricular perfusion imaging agent, 25 normal volunteers and 25 patients with suspected coronary disease were studied with both sestamibi and thallium-201 SPECT. All patients underwent cardiac characterization. Compared to thallium-201 images, visualization of the right ventricle was superior for sestamibi in all cases. After computer masking of the left ventricle, count profiles for each 6-mm right ventricular short-axis slice were extracted and plotted in a bull's-eye type polar map with images normalized to maximal right ventricular counts. On sestamibi right ventricular polar maps, 7 of 11 patients (64%) with right coronary stenosis had fixed or reversible inferior right ventricular defects. None of the 25 volunteers or patients without right coronary stenosis had right ventricular defects (true-negative rate = 100%). We conclude that sestamibi SPECT provides an accurate means to assess right ventricular regional perfusion, with data presentation and interpretation facilitated by the polar map display.

J Nucl Med 1991; 32:1199–1205

Ischemia and infarction of the right ventricle occur in patients with right coronary artery disease. Right ventricular ischemia precipitated by exercise or other types of stress is very infrequently diagnosed by existing methodology. However, the identification of the presence and extent of right ventricular ischemia may be helpful both to identify the presence of right coronary artery disease and to better quantify the extent of jeopardized myocardium and the significance of right coronary artery lesions.

Right ventricular infarction occurs frequently, but often remains undiagnosed. In patients with fatal myocardial infarction, right ventricular involvement is common, reported to occur in as many as 50% of patients (*1*). In patients with nonfatal infarcts, right ventricular infarction is associated with significant morbidity, including an increased incidence of arrhythmias, systemic hypoperfusion, and right heart failure. Unlike patients with infarction confined to the left ventricle, those with right ventricular infarction frequently require volume expansion to maintain systemic perfusion pressure. Therefore, because of the frequency of right ventricular infarction, the increased associated morbidity, and the therapeutic implications, identification of right ventricular infarction is important clinically.

Technetium 99m-labeled isonitriles localize in the right ventricular myocardium following injections either at rest or during exercise. We and other investigators have observed that right ventricular visualization with ^{99m}Tc-sestamibi is greater than with ^{201}Tl.

The purpose of this study was to evaluate the clinical applicability of exercise and resting sestamibi SPECT myocardial perfusion imaging in identifying regional right ventricular ischemia and infarction. Means to optimize right ventricular myocardial visualization were tested, including computer masking of activity in the left ventricle and the development of a two-dimensional polar coordinate map display of three-dimensional right ventricular SPECT date. The diagnostic accuracy of the technique in identifying right ventricular perfusion abnormalities associated with right coronary artery disease was assessed in normal volunteers and patients with angiographically documented coronary disease.

METHODS

Study Population: Patients and Normal Volunteers

The study population consisted of 25 normal volunteers and 25 patients suspected of having coronary artery disease who were referred to the nuclear medicine laboratory for exercise myocardial perfusion imaging. The 25 normal volunteers included 13 women and 12 men, each with a <1% likelihood of coronary disease determined by analysis of risk factors. Their mean age was 36 yr. Among the 25 patients studied, there were 5 women and 20 men, with a mean age of 59 yr. All patients underwent coronary arteriography within 5 days of radionuclide imaging. Coronary artery disease, defined as ≥ 50% luminal diameter narrowing of one or more coronary arteries, was present in 19 of the 25 patients. There was ≥ 50% stenosis of ther right coronary artery in 11 of these patients. Three patients had a history and electrocardiographic evidence of inferior myocardial infarction.

Received Jul. 5, 1990; revision accepted Nov. 19, 1990.

For reprints contact: E. Gordon DePuey, MD, Department of Nuclear Medicine, St. Luke's-Roosevelt Hospital, Amsterdam Avenue at 114th St., New York, NY 10025.

* Current address: St. Luke's-Roosevelt Hospital Center, New York, NY.

In each case, the event occurred more than 6 mo previously. In no case, had there been signs or symptoms or imaging data (echocardiography, ^{99m}Tc-pyrophosphate scan, or radionuclide angiocardiography) to suggest right ventricular infarction.

Imaging Protocols

This protocol was approved by the Emory Institutional Review Board and Radiation Safety Committee. All subjects granted written informed consent to participate in the study.

All volunteers and patients underwent exercise myocardial perfusion imaging with both ^{201}Tl and ^{99m}Tc-sestamibi. In all cases, thallium scans were performed first, with sestamibi studies performed within the subsequent 3 days.

Thallium SPECT imaging was performed using our standard clinical protocol. Thallium (3.5 mCi) was injected at peak treadmill exercise. Image acquisitions were performed at 10 min and at 3–4 hr. A 180-degree imaging arc of 32 views, 40 sec each, was used, extending from the 45-degree right anterior oblique to 45-degree left posterior oblique position. Short-axis, vertical long-axis, and horizontal long-axis 6-mm tomographic slices oriented parallel to and perpendicular to the long-axis of the left ventricle were reconstructed using filtered backprojection and a Ramp-Hanning filter with a 0.82 cycles/cm cutoff frequency.

A two-day protocol was used for the sestamibi studies. The exercise study was performed on Day 1. Subjects had fasted for at least 4 hr. Fifteen millicuries were injected at peak treadmill exercise at a maximum heart rate within 5% of that achieved for the previous thallium study. Subjects then drank 10 oz of milk to promote hepatic excretion of the radiotracer, and SPECT imaging was begun at 90–120 min, in most cases closer to 120 min. The following day, 15 mCi were injected at rest with subjects again fasting for at least 4 hr. Subjects then drank 10 oz of milk, and SPECT imaging was begun at 90–120 min, again usually closer to 120 min.

Sestamibi SPECT studies were acquired and processed using the identical parameters as those for ^{201}Tl except for a 20% ^{99m}Tc energy window. In this study, no attempt was made to optimize image acquisition and processing for the higher count density, higher spatial resolution ^{99m}Tc studies.

Subjective and Objective Analysis of Right Ventricular Image Quality

For ^{201}Tl and ^{99m}Tc-sestamibi SPECT, right ventricular images were compared both subjectively and objectively. For subjective analysis, an experienced nuclear medicine physician viewed ^{201}Tl and ^{99m}Tc-sestamibi studies side by side. Images were compared with regard to the right ventricular myocardium-to-background ratio and the ability to delineate the right ventricular cavity and myocardium. These comparisons were made for both exercise and resting/delayed images.

For objective analysis, the ratio of maximum counts in the right and left ventricles was determined at the mid-ventricular level, using a count rate profile extending across the short-axis tomographic slice in which the right ventricle was best visualized.

Because right ventricular visualization was invariably better with ^{99m}Tc-sestamibi than with ^{201}Tl, as noted below in the Results section, and because definition of the right ventricle with ^{201}Tl was so poor, further image processing was performed for only the sestamibi images.

Optimized Right Ventricular Visualization by Computer Image Masking

Right ventricular visualization can be enhanced by masking left ventricular activity and thereby enhancing contrast in the lower count environment of the right ventricle. First, a short-axis slice is selected in which the right ventricle and its cavity are best visualized (Fig. 1). The operator then draws a generous region of interest, which includes the entire left ventricle and also any background activity in the left hemithorax or abdominal viscera (Fig. 2). All activity in the selected region of interest is then masked (i.e., set to zero counts). Masking is performed for this slice and by the computer for all other short-axis slices. A similar masking routine is used for both exercise and resting sestamibi images. After the masking process, 6-mm thick short-axis slices of the right ventricle for exercise and resting studies can be displayed at multiple levels (Fig. 3). The right ventricle can also be visualized in vertical long-axis slices oriented parallel to the long-axis of the left ventricle. The vertical long-axis display of the right ventricle does not require computer masking of the left ventricle.

Construction of a Right Ventricular Polar Coordinate Map

To further optimize the display of sestamibi right ventricular perfusion images, we developed a polar coordinate map display. For exercise and resting images, the apex and base of the right ventricle are selected using cursors placed on the horizontal long-axis slice at mid-left ventricular level. As the cursor is positioned, the corresponding short-axis view of the right ventricle is displayed in which all left ventricular activity has been eliminated by the masking routine previously described. In selecting the basal limit, care must be taken to confine the slice only to the right ventricle and not to include the relatively count-poor right atrium.

Similar to the method routinely used for the left ventricle bull's-eye reconstruction, in the mid-right ventricular short-axis slice, the center of the right ventricle is defined, usually as a point midway between the medial limits of the anterior and inferior walls. The maximal count density in the right ventricle along radians constructed every 9 degrees is determined. A box is placed by the operator which will limit the radius of search, thereby decreasing the possibility of including counts from adjacent background and visceral structures. Circumferential profiles are thereby determined for each right ventricular short-axis slice.

FIGURE 1. Six-millimeter thick short-axis exercise sestamibi tomographic slice at the level of mid-right ventricular cavity. Image intensity is greater than that used for routine display of left ventricular perfusion in order to optimally display the right ventricular myocardium.

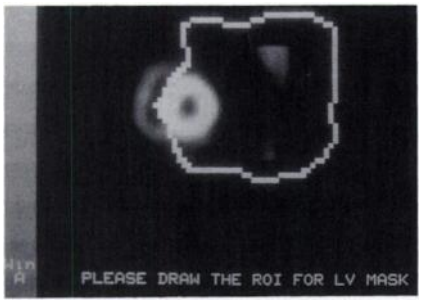

FIGURE 2. Operator-defined region of interest used to exclude left ventricular and background activity.

These circumferential profiles are replotted in polar coordinates and positioned in a "bull's-eye" plot. Each plot is normalized to maximal count density and color-coded (Fig. 4).

RESULTS

Comparison of ^{201}Tl and ^{99m}Tc-Sestamibi Images

In both the exercise and resting/delayed images, right ventricular visualization was subjectively judged superior with ^{99m}Tc-sestamibi in all volunteers and in all patients. In the resting sestamibi SPECT studies, images were deemed adequate for evaluation of the right ventricle in all patients and in 22 of the 25 volunteers. In the three subjects in whom right ventricular visualization in the resting study was judged suboptimal, there was considerable tracer activity in abdominal viscera immediately adjacent to the diaphragmatic surface of the right ventricle. Two of these three resting studies were judged uninterpretable.

Using count rate profiles at the mid-ventricular level, extending across the short-axis tomographic slice in which the right ventricle was best visualized, the ratio of maximum counts in the right and left ventricles was determined. The right-to-left ventricular count ratio was not significantly different for ^{201}Tl and sestamibi, with a mean right-to-left ventricular ratio for either radiopharmaceutical of 1 to 3.5 (Fig. 5).

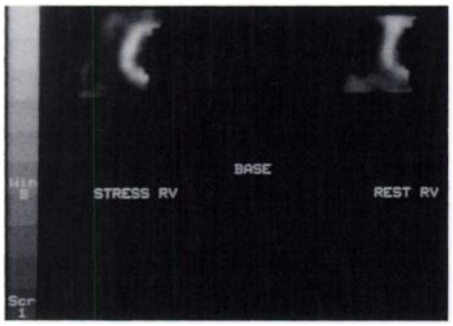

FIGURE 3. After masking of left ventricular pixels, isolated short-axis tomographic right ventricular slices are displayed. Note relatively greater tracer concentration in the liver, adjacent to the inferior wall of the right ventricle in the resting image.

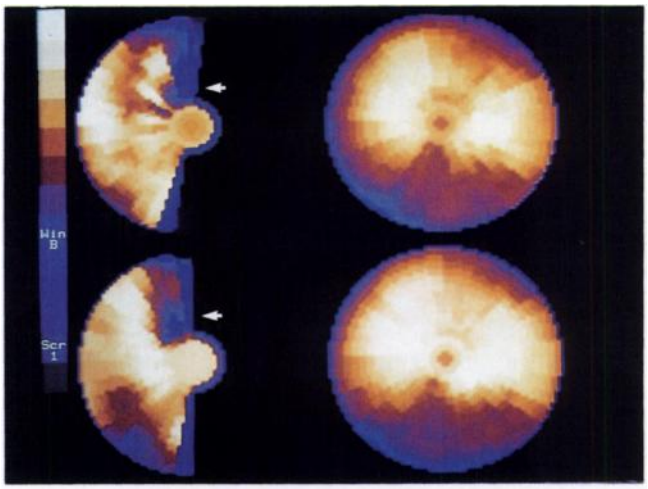

FIGURE 4. Exercise (top) and resting (bottom) left ventricular (right) and right ventricular (left) color-coded polar coordinate maps. In the left ventricular bull's-eye maps, tracer distribution is physiologic, and moderate inferior attenuation is present due to the left hemidiaphragm in this normal male volunteer. Normal tracer distribution is present throughout the right ventricular myocardium. Some differences in tracer distribution are noted at the periphery of the right ventricular polar map due to imprecision in identification of the tricuspid valve plane and selection of the base of the right ventricle. Likewise, imprecision in selection of the apex, the finite thickness of the 6-mm tomographic slice, and inclusion of a position of the interventricular septum in the apical slice result in apparent differences in apical count density. A consistent finding in sestamibi right ventricular images is decreased tracer concentration in the anterior wall, corresponding to the location of the pulmonary outflow tract (arrows).

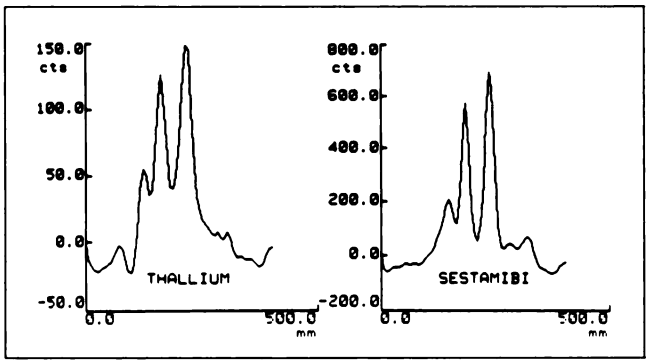

FIGURE 5. Count rate profiles for ^{201}Tl (left) and ^{99m}Tc-sestamibi (right) exercise images in a normal volunteer subject derived from a 1-pixel (6.4 mm) thick region of interest extending horizontally across the heart at mid-ventricular level. For either curve, moving from left to right, the three peaks represent the free wall of the right ventricle, the interventricular septum, and the posterolateral wall of the left ventricle, respectively. The counts per pixel (y-axis) demonstrate a four-fold increase in myocardial count density with ^{99m}Tc-sestamibi. The peak right-to-left-ventricular count density ratios are similar for thallium (1:3.0) and sestamibi (1:3.5). There is better definition of the left and right ventricular cavities with sestamibi.

Correlation of ^{99m}Tc-Sestamibi SPECT with Coronary Angiography

All studies were interpreted by visual inspection of both the tomographic slices and bull's-eye plots. In the 25 normal volunteers, left and right ventricular images were normal at exercise in all cases and at rest in the 23 studies deemed interpretable. In the six patients with normal coronary arteries, left and right ventricular images were likewise all normal. In the eight patients with coronary disease not involving the right coronary artery, left ventricular defects were present in six, or 75%, which were reversible in three; however, the right ventricle appeared normal in all these cases.

In the 11 patients with right coronary stenosis, left ventricular defects were also present in 10, or 91%, with reversibility in 4. Seven of these 11 patients also had exercise right ventricular perfusion defects with reversibility in 3. Right coronary lesions were proximal in six of these seven cases. In the seventh case, the stenosis involved the mid-portion of the right coronary artery, but a lesion was also identified at the origin of the right ventricular branch. In the two cases with defects involving only the left ventricle, stenosis involved the mid-right coronary artery, distal to the origin of right ventricular branches. Results are summarized in Table 1.

Case Examples

Case 1 (Fig. 6). This 60-yr-old man (patient JH in Table 1) had sustained an inferior myocardial infarction. A relatively small, fixed inferolateral perfusion defect is present in the left ventricular bull's-eye images. However, there is a more sizable perfusion defect involving the inferior wall of the right ventricle noted in the exercise images, which is somewhat more marked and extensive in the resting study. Coronary angiography demonstrated a proximal right coronary artery occlusion and inferior left and right ventricular hypokinesis.

Case 2 (Fig. 7). This 40-yr-old man (patient JC in Table 1) had also sustained an inferior myocardial infarction, which is apparent by the large inferolateral defect present in the left ventricular exercise bull's-eye plot. There is evidence of slight reperfusion in the resting image. However, in the exercise right ventricular bull's-eye plot, there is a large inferior perfusion defect, which normalizes in the resting image. This patient's exercise electrocardiogram was negative for ischemia. At coronary angiography, he was found to have proximal right coronary artery stenosis.

DISCUSSION

The diagnosis of right ventricular myocardial infarction is clinically important since patients with right ventricular infarction complicating left ventricular infarction have an increased incidence of arrhythmias, systemic hypoperfusion and signs of right-sided heart failure (*2*). Identification of such patients is important because their appropriate clinical management usually includes vigorous volume loading in contrast to patients with isolated left ventricular infarction in whom preload and afterload reduction is routine.

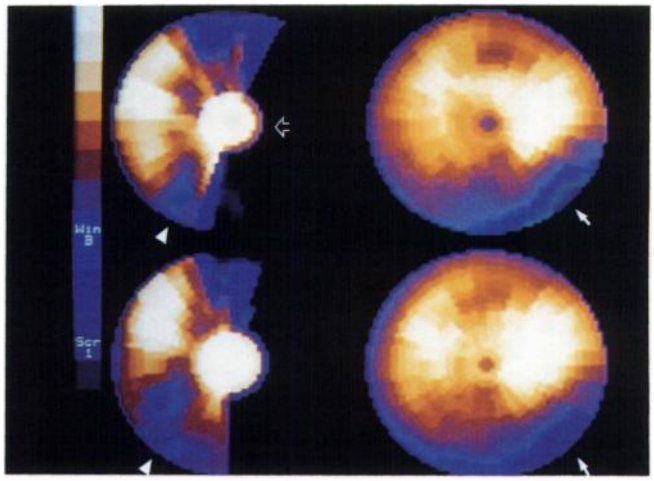

FIGURE 6. Fixed inferior left (solid arrows) and right (arrowheads) ventricular perfusion defects. See description in text, Case 1. Note the very intense apex (open arrows), a normal variant in right ventricular sestamibi images.

Right ventricular infarction is commonly associated with left ventricular infarction. Andersen et al. reported a series of 107 consecutive autopsies performed on patients dying of myocardial infarction. Of 214 regional infarcts identified, right ventricular infarction was present in 50% (*1*). Right ventricular infarction most frequently involves the inferoposterior free wall and the posterior septum. Right ventricular infarction occurred with equal frequency in patients with anterior and inferoposterior left ventricular infarction. However, right ventricular involvement was much greater with inferoposterior infarction, on the average involving 15% of the right ventricular myocardium, whereas right ventricular infarcts associated with anterior

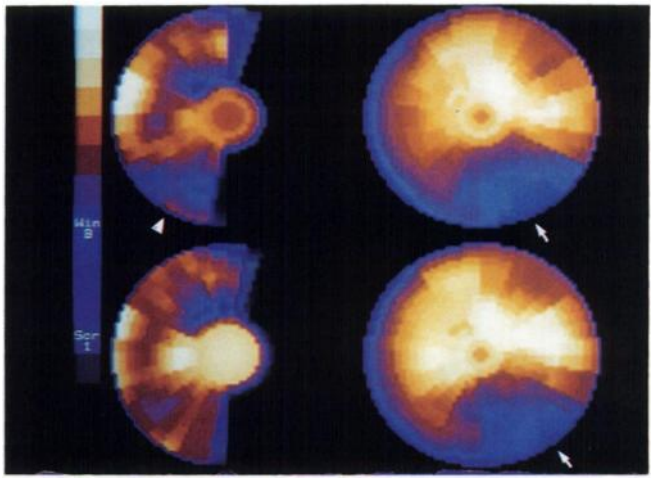

FIGURE 7. Fixed inferolateral left ventricular perfusion defect (solid arrows) and reversible inferior right ventricular defect (arrowhead). See description in text, Case 2.

TABLE 1
Sestamibi SPECT Findings in 11 Patients with ≥50% Right Coronary Artery Stenosis

Patient	% RCA stenosis	Location	Prior IWMI	RV defect	LV defect
HW	70%	proximal	no	reversible	reversible
DS	80%	mid + RV branch	no	fixed	fixed
CV	50%*	proximal	no	fixed	fixed
JB	70%	mid	yes	no	fixed
RE	100%	proximal	no	reversible	reversible
ES	50%	proximal	no	no	no
LR	100%	proximal	no	no	reversible
JC	65%	proximal	yes	fixed	fixed
LM	50%*	distal	no	no	fixed
JH	100%	proximal	yes	reversible	reversible
WR	50%	proximal	no	fixed	fixed

* Status post-right coronary artery percutaneous transluminal coronary angioplasty.
IWMI = Q-wave inferior wall myocardial infarction; LV = left ventricle; RCA = right coronary artery; and RV = right ventricle.

infarcts involved an average of only 1% of the right ventricular myocardium. Therefore, in patients with inferior wall infarction, significant right ventricular extension is a frequent finding, occurring in 66% of Andersen's autopsy series. Another autopsy series by Isner et al. reported a significant but lower incidence of 14% (*3*). The more proximal the location of the right coronary occlusion, the greater the damage to the right ventricle (*4*). Right coronary occlusion distal to all right ventricular wall branches results in no right ventricular infarction. Other factors that may predispose patients to right ventricular infarction include acute right ventricular pressure and/or volume overload (*5*) and right ventricular hypertrophy (*6*).

Clinically, right ventricular infarction is frequently unsuspected. Classical signs of right heart failure, including a distended jugular venous pulse and a positive Kussmaul's sign in the absence of the left heart failure, are both insensitive and nonspecific for right ventricular infarction. Dell'Italia et al. observed these findings in 4 of 8 patients with documented right ventricular infarction and 8 of 45 patients without infarction (*7*). Standard 12-lead electrocardiographic examination usually cannot diagnose right ventricular infarction. However, with specially placed right precordial leads, 1–5 mm ST segment elevation has been observed in 70%–100% of patients with right ventricular infarction (*2,8*). Hemodynamic measurements documenting right atrial pressure nearly equal to or higher than pulmonary capillary wedge pressure and a severely noncompliant pattern on the right atrial pressure tracing (y descent deeper than x descent) were observed by Lopez-Sendon et al. in 82% of patients with documented right ventricular infarction (*9*). Other clinical indicators are less reliable. There may be radiographic evidence of a right pleural effusion despite clear lung fields and a normal pulmonary capillary wedge pressure (*10*). A markedly elevated peak serum creatine kinase (>2000 U) despite electrocardiographic evidence of acute infarction involving only the inferior wall also may suggest right ventricular involvement (*11*).

Imaging modalities currently available to diagnose and evaluate right ventricular myocardial infarction include two-dimensional echocardiography, ^{99m}Tc-pyrophosphate scintigraphy, and first-pass or equilibrium radionuclide angiocardiography. The presence of a right ventricular regional wall abnormality on two-dimensional echocardiography was reported by Lopez-Sendon et al. to be 84% sensitive and 90% specific for right ventricular infarction (*12*). With radionuclide ventriculography, numerous authors have demonstrated depressed right ventricular ejection fraction in patients with right ventricular infarction (*2*). Starling found mean right ventricular ejection fraction to be 28% in patients with right ventricular infarction versus 44% in those without infarction (*13*). Regional right ventricular wall motion abnormalities in radionuclide ventriculography are most frequently associated with right ventricular infarction (*14*). In addition to depressed global and regional right ventricular function, a coexistent decrease in left ventricular end-diastolic volume, stroke index, and cardiac index are additional test parameters to support the diagnosis of right ventricular infarction (*15*).

Tobinick et al. demonstrated right ventricular ^{99m}Tc-pyrophosphate uptake in 7 of 17 patients (41%) with scintigraphically apparent left ventricular inferior infarcts (*16*). Using hemodynamic measurements as a gold standard, Sharpe et al. demonstrated focal uptake in 83% of patients with right ventricular infarction (*17*).

Due to limited ability to visualize the right ventricular myocardium, evaluation of exercise-induced right ventricular perfusion defects with ^{201}Tl has been difficult. Using planar methodology, Brown et al. observed transient ^{201}Tl defects in right ventricular tracer distribution following exercise in 8 of 55 patients with right and/or posterior descending coronary artery disease (*18*). There was non-

visualization of the right ventricle in an additional 9 of those 55 patients. In 43 of the 55 patients studied with proximal stenosis, right ventricular defects occurred less frequently than inferior left ventricular defects (35% versus 70%). A case report by Kottler et al. described a resting SPECT ^{201}Tl study, which demonstrated a large inferior perfusion defect involving both the left and right ventricles in a patient with a clinically documented inferior infarct with right ventricular extension (*19*). However, we are aware of no sizable series of patients in whom right ventricular perfusion was evaluated with ^{201}Tl SPECT.

Studies to date have used worsening of global and/or regional right ventricular function as a marker of right ventricular ischemia. In patients who fail to increase right ventricular ejection fraction during exercise, there is an increased incidence of proximal right coronary artery stenosis (*20,21*). However, a decrease in right ventricular ejection fraction during exercise is a very nonspecific indicator of right coronary disease, since any cause of increased right ventricular afterload, including pulmonary hypertension, chronic obstructive pulmonary disease, and left ventricular dysfunction, may alter right heart performance (*22,23*). A localized exercise-induced wall motion abnormality may be a more specific indicator of right coronary artery disease. However, investigators have noted that not even regional right ventricular dysfunction is a specific indicator of right coronary artery stenosis (*24*).

In the present study, right ventricular defects were identified only in patients with right coronary artery disease with angiographic lesions usually present proximal to or involving the right ventricular branch(es). Of the 11 patients we studied who had right coronary disease, 7 (64%) had right ventricular perfusion defects, 3 of which were reversible, and 4 of which were fixed. This incidence of right ventricular involvement is similar to the 50% incidence of right ventricular involvement reported in Andersen's autopsy series of patients dying from acute myocardial infarction (*1*). In the present study although the ability to image the right ventricle with ^{99m}Tc-sestamibi and the concordance of image findings and coronary arteriography is documented, no inferences regarding the actual sensitivity or specificity of the technique in detecting right ventricular infarction or ischemia can be made.

Using planar ^{201}Tl exercise imaging, Gutman et al. observed an additive sensitivity of the presence of inferior left ventricular and right ventricular defects in identifying patients with proximal right coronary artery stenosis (*25*). The sensitivity and specificity of a right ventricular defect were 59% and 88%, and those for an inferior left ventricular defect were 67% and 68%. For an abnormality involving either the right or left ventricle, the sensitivity and specificity were 93% and 56%, respectively.

In contrast, test sensitivity of an inferior left ventricular perfusion abnormality in detecting right coronary artery disease with ^{201}Tl and ^{99m}Tc-sestamibi SPECT is well recognized to be excellent, approaching 90% in most reported studies. It is doubtful that identification of right ventricular perfusion defects will further improve test sensitivity, since most right ventricular perfusion defects are accompanied by larger left ventricular regional abnormalities. However, it is possible that test specificity would improve in patients who demonstrate coexistent left and right ventricular perfusion defects.

SPECT image acquisition modifications will most likely further improve ^{99m}Tc-sestamibi right ventricular perfusion images. A high-resolution collimator can be used since the associated decrease in count density will still allow for adequate counting statistics. Gated acquisition can provide end-diastolic images which maximize right ventricular volume and minimize image degradation due to cardiac motion and contraction, thereby improving defect identification. Display of multi-frame gated perfusion images in endless loop cinematic format allows for the simultaneous assessment of right ventricular perfusion and function. An alternate means to evaluate right ventricular perfusion and function with a single injection of ^{99m}Tc-sestamibi is by performing first-pass radionuclide angiography at the time of tracer injection with perfusion imaging at a delayed interval. The presence of a regional right ventricular wall motion abnormality corresponding in location to the site of a perfusion defect will most likely increase the specificity of both findings for the presence of localized infarction.

In the present study, the SPECT imaging arc was 180 degrees, extending from the 45-degree right anterior oblique to the 45-degree left posterior oblique angle, optimized for left ventricular imaging. Perhaps extension of this arc from the right lateral to the 45-degree left posterior oblique view (225 degrees) will further improve right ventricular visualization.

For right ventricular polar coordinate map reconstruction, masked short-axis slices of the right ventricle were used. The precise definition of the right ventricular apex and base (tricuspid valve plane) requires a moderate degree of operator skill and experience. As with construction of left ventricular bull's-eye plots, incorrect slice selection, particularly at the apex and base, can create polar map artifacts. Alternately, the horizontal long-axis at the mid-right ventricular level, in which the apex and base are more clearly delineated, could be used for slice selection.

In the present study, no attempt was made to quantify right ventricular perfusion defects by comparison of patient data to normal files. With enrollment of a larger number of normal control subjects this should be possible in the future. Moreover, the reproducibility of the technique should be established using quantitative analysis.

SUMMARY

SPECT imaging with ^{99m}Tc-sestamibi provides a useful means to evaluate regional right ventricular perfusion. The display and analysis of right ventricular images is enhanced by computer masking of left ventricular activity and polar coordinate mapping. In a small series of volunteer subjects,

the technique is highly specific for the identification of perfusion defects in patients with right coronary artery disease. Fixed or reversible right ventricular regional perfusion defects were identified in 64% of patients with right coronary artery disease.

REFERENCES

1. Andersen HR, Falk E, Nielsen D. Right ventricular infarction: frequency size and topography in coronary disease: a prospective study comprising 107 consecutive autopsies from a coronary care unit. *J Am Coll Cardiol* 1987;10:1223–1232.
2. Isner JM. Right ventricular myocardial infarction. *JAMA* 1988;259:712–718.
3. Isner JM, Roberts WC. Right ventricular infarction complicating left ventricular infarction secondary to coronary heart disease; frequency, location-associated findings and significance from analysis of 236 necropsy patients with acute or healed myocardial infarction. *Am J Cardiol* 1978;42:885–894.
4. Weinshel AJ, Isner JM, Salem DN, et al. The coronary anatomy of right ventricular myocardial infarction: relationship between the site of right ventricular occlusion and origin of the right ventricular free wall branches [Abstract]. *Circulation* 1983;68:351.
5. King TC, Saffitz JE. Acute right ventricular infarction resulting from intracardiac infusion of hyperosmotic hyperalimentation solution. *Am J Cardiol* 1985;55:1659–1660.
6. Forman MB, Wilson BH, Sheller JR, et al. Right ventricular hypertrophy is an important determinant of right ventricular infarction complicating acute inferior left ventricular infarction. *J Am Coll Cardiol* 1987;10:1180–1187.
7. Dell'Italia LJ, Starling MR, O'Rourke RA. Physical examination for exclusion of hemodynamically important right ventricular infarction. *Ann Intern Med* 1983;99:608–611.
8. Erhardt LR, Sjogren A, Wahlbert I. Single right-sided precordial lead in the diagnosis of right ventricular involvement in inferior myocardial infarction. *Am Heart J* 1976;91:571–576.
9. Lopez-Sendon J, Coma-Canella I, Gamallo C. Sensitivity and specificity of hemodynamic criteria in the diagnosis of acute right ventricular infarction. *Circulation* 1981;64:515–525.
10. Lorell B, Leinbach RC, Pohost GM, et al. Right ventricular infarction: clinical diagnosis and differentiation from cardiac tamponade and pericardial constriction. *Am J Cardiol* 1979;43:465–471.
11. Strauss HD, Sobel BE, Roberts R. The influence of occult right ventricular infarction on enzymatically estimated infarct size, hemodynamics and prognosis. *Circulation* 1980;62:503–508.
12. Lopez-Sendon J, Garcia-Fernandez MA, Coma-Canella I, et al. Segmental right ventricular function after acute myocardial infarction: two-dimensional echocardiographic study in 63 patients. *Am J Cardiol* 1983;51:390–396.
13. Starling MR, Dell'Italia LJ, Chaudhuri TK, et al. First transit and equilibrium radionuclide angiography in patients with inferior transmural myocardial infarction: criteria for the diagnosis of associated hemodynamically significant right ventricular infarction. *J Am Coll Cardiol* 1984;5:923–930.
14. Ratner SJ, Huang PJ, Friedman MI, et al. Assessment of right ventricular anatomy and function by quantitative radionuclide ventriculography. *J Am Coll Cardiol* 1989;13:354–359.
15. Shah PK, Maddahi J, Berman DS, et al. Scintigraphically detected predominant right ventricular dysfunction in acute myocardial infarction: clinical and hemodynamic correlates and implications for therapy and prognosis. *J Am Coll Cardiol* 1985;6:1264–1272.
16. Tobinick E, Schelbert HR, Henning H, et al. Right ventricular ejection fraction in patients with acute myocardial infarction: two-dimensional echocardiographic study in 63 patients. *Am J Cardiol* 1983;51:390–396.
17. Sharpe DN, Botvinick EH, Shames EM, et al. The noninvasive diagnosis of right ventricular infarction. *Circulation* 1978;57:483–490.
18. Brown KA, Boucher CA, Okada RD, et al. Serial right ventricular thallium-201 imaging after exercise: relation to anatomy of the right coronary artery. *Am J Cardiol* 1982;50:1217–1222.
19. Kottler J, Trobaugh GB, Williams DL, et al. Demonstration of a right ventricular infarction with tomographic thallium myocardial imaging. *J Nucl Med* 1982;23:1111–1113.
20. Johnson LL, McCarthy DM, Sciacca RR, et al. Right ventricular ejection fraction during exercise in patients with coronary artery disease. *Circulation* 1979;60:1284–1291.
21. Maddahi J, Berman DS, Matsouka DT, et al. Right ventricular ejection fraction during exercise in normal subjects and in coronary artery disease patients: assessment by multiple-gated equlibrium scintigraphy. *Circulation* 1980;62:133–140.
22. Berger HJ, Matthay RA, Davies RA, et al. Comparison of exercise right ventricular performance in chronic obstructive pulmonary disease and coronary artery disease: noninvasive assessment by quantitative radionuclide angiocardiography. *Invest Radiol* 1979;14:342–353.
23. Weiner BH, Alpert JS, Dalen JE, et al. Response of the right ventricle to exercise in patients with chronic heart disease. *Am Heart J* 1983;105:386–392.
24. Ratner SJ, Friedman MI, Pierson RN, et al. Incidence of exertional right ventricular wall motion abnormalities in patients with coronary artery disease. *Clin Cardiol* 1988;239–244.
25. Gutman J, Brachman M, Rozanski A, et al. Enhanced detection of proximal right coronary artery stenosis with the additional analysis of right ventricular thallium-201 uptake in stress scintigrams. *Am J Cardiol* 1983;51:1256–1260.